Helsinki University of Technology
Department of Electrical and Communications Engineering
Espoo 2004

Characterization Methods for

Silicon Photodiode and Silicon Sub-Surface Properties

Atte Haapalinna

Dissertation for the degree of Doctor of Science in Technology to be presented with due permission of the Department of Electrical and Communications Engineering, Helsinki University of Technology, for public examination and debate in Auditorium S4 at Helsinki University of Technology (Espoo, Finland) on the17[th] of December, 2004, at 12 o'clock noon

Helsinki University of Technology
Department of Electrical and Communications Engineering
Metrology Research Institute

Teknillinen korkeakoulu
Sähkö-ja tietoliikennetekniikan osasto
Mittaustekniikan laboratorio

ABSTRACT OF DOCTORAL DISSERTATION

Author   Atte Haapalinna

Name of the dissertation

Characterization Methods for Silicon Photodiode and Silicon Sub-Surface Properties

Date of manuscript	Date of the dissertation December 17th, 2004
☐ Monograph	☑ Article dissertation (summary + original articles)

Abstract

This thesis considers the characterization of silicon photodiode and the applications of silicon photodiodes in precision metrology, and some aspects of the silicon material characterizations. Such material characterizations are required in the process of semiconductor device manufacturing, one example of which is the silicon photodiode manufacturing.

The motivation for the research on radiometry reported in this thesis has been the development of optical metrology at the Helsinki University of Technology (HUT). Most of the applications for this research are found in the UV-metrology. Importance of the UV-metrology arises from the environmental importance of accurate gauging of optical power at these wavelengths.

This thesis describes the derivation and experimental verification of simple mathematical models, based on Fresnel equations. These models have allowed significant reductions in the uncertainties of spectrophotometric and radiometric measurements, especially in the UV wavelengths. These measurements are carried out using silicon photodiode-based detection systems. The reductions achieved in the measurement uncertainties have been utilized in the detector-based realizations of optical quantities maintained as national standards at HUT.

The structure and operating principle of silicon photodiodes brings up the process of manufacturing of these devices, and the material characterizations required during this process. Novel methods in machining of silicon wafers for semiconductor industry pose new challenges for these characterizations. One such challenge is the need to characterize sub-surface damage in silicon wafers, induced by abrasive machining. The measurement of the sub-surface damage in silicon was the goal set for the work on materials characterization reported here. Various potential solutions to this requirement have been studied in this thesis, some of which are based on the spectrophotometric research carried out at HUT. Complete solution to this requirement has not been found. This thesis compares a number of promising methods and combines their respective advantages in order to create a more comprehensive understanding on the subject under study.

Keywords   photodiode, silicon, radiometry, sub-surface damage, linearity, reflectance

Preface

The research presented in this thesis has been carried out at these two institutes: Metrology Research Institute of Helsinki University of Technology (MRI-HUT) and Fraunhofer Institut für Produktionstechnologie (IPT), to which I was appointed by my current employer, Okmetic, during 2001.

I wish to express my gratitude to my supervisor, professor Erkki Ikonen, for his encouragement, guidance, and above all, unrelenting faith in the successful completion of this work.

I am grateful for the valuable contribution of Dietmar Pähler and also all the other colleagues at the IPT, Aachen, both for their considerable scientific input, and the motivation and fine example they provided.

My research has been part of a team effort, and I want to thank all my co-authors and colleagues, especially Farshid Manoochehri, Petri Kärhä, Saulius Nevas and Pasi Toivanen

The contribution of Seppo Metsälä in the excellent workmanship and valuable guidance in manufacturing the required experimental set-ups has been paramount in achieving the results reported

Funding of my research at the MRI-HUT was enabled through the Graduate School of Modern Optics and Photonics, which is acknowledged with gratitude. I appreciate also the financial support by the Centre for Metrology and Accrediation (MIKES).

I have been fortunate in having an employer, Okmetic, that has had a positive attitude towards scientific research. Most importantly, Okmetic has provided me with the opportunity to work at the IPT and, as a direct consequence, to finish my thesis.

Finally, I am grateful for my wife, Satu and my two precious daughters, Katri and Aino, for their love, understanding and balance they have provided me during these years.

List of publications

This thesis consists of an overview and the following selection of the author's publications.

I.   A. Haapalinna, F. Manoochehri and E. Ikonen, "High-accuracy measurement of specular reflectance and transmittance," Analytica Chimica Acta, **380**, 317-325 (1999).
II.   A. Haapalinna, S. Nevas, F. Manoochehri and E. Ikonen, "Precision spectrometer for measurement of specular reflectance," Review of Scientific Instruments **73**, 2237-2242 (2002).
III.   A. Haapalinna, P. Kärhä and E. Ikonen, "Spectral reflectance of silicon photodiodes," Applied Optics **37**, 729-732 (1998).
IV.   A. Haapalinna, T. Kübarsepp, P. Kärhä and E. Ikonen, "Measurement of absolute linearity of photodetectors with a diode laser," Measurement Science and Technology **10**, 1075-1078 (1999).
V.   T. Kübarsepp, A. Haapalinna, P. Kärhä and E. Ikonen, "Nonlinearity measurements of silicon photodetectors," Applied Optics **37**, 2716-2722 (1998).
VI.   P. Kärhä, A. Haapalinna, P. Toivanen, F. Manoochehri and E. Ikonen, "Filter radiometry based on direct utilization of trap detectors," Metrologia **35,** 255-259 (1998).
VII.   A. Haapalinna, S. Nevas and D. Pähler, "Rotational grinding of silicon wafers – Sub-surface damage inspection", Materials Science and Engineering B **107**, 321-331(2004).
VIII.   F. Klocke, D. Pähler, A. Haapalinna and A. Jacob, "Rotational grinding is solution to surface damages," Proc. SEMICON West 2003, ISBN 1-892568-78-0 (2003).

Author's contribution

All the publications included in this thesis are products of teamwork of the contributing authors.

The author of this thesis has designed and constructed the reflectance accessory for the HUT reference spectrometer. The test measurements and their validation with respect to theoretical calculations were carried out by the author [I]. He carried out the development and uncertainty analysis of the reflectance accessory reported in publication [II]. He developed the measurement procedures and carried out the actual measurements reported in publication [III].

The author actively participated to the project aimed at characterizing the linearity of silicon photodiodes used for precision radiometry at HUT. He carried out the development, characterization and analysis of the measurement system described in publication [IV]. He participated in the characterizations and contributed to the analyses, which have been reported in publication [V].

The author has contributed to the research aimed at improving the methods of filter radiometry by characterizing the reflectance of the interference filters used in filter radiometers. The author also characterized and improved the efficiency of the thermal stabilization used to minimize the measurement uncertainty of the filter radiometer reported in publication [VI], for which he also carried out the direct responsivity characterization.

The author held the main responsibility in formulating the comparison study of alternative characterization methods for sub-surface damages in machined single-crystal silicon. He participated in the sample preparation process required by the study, and he carried out most of the measurements used in the comparison. He carried out the analysis of the comparison study, reported in publication [VII]. He has contributed to the analysis reported in publication [VIII].

The author prepared the manuscripts for publications [I, II, III, V and VII].

CONTENTS

1. Introduction

The growth of high technology and, in particular, the growth of electronics industry has changed the world. The sector of electronic systems and devices is the largest industrial sector in the international trade. The central building block behind this development is single crystal silicon, which in the form of semiconductor devices built on silicon wafers forms an increasing part of the vast electronics market. The world market for semiconductors is currently around 200 000 million USD, some 5% of which is the share of optoelectronic devices [1].

Extensive studies have been carried out to characterize the behavior of single crystal silicon. Even today, some thirty years after the introduction the first integrated circuit, increasing sophistication of silicon-based semiconductor manufacturing and novel approaches required by the rapid development give rise to considerable body of research, both in applications to practical problems and in the form of more basic research. One emerging field of silicon microelectronics, called microphotonics [2], combines photonics and silicon microelectronic components. This combination holds promise of bypassing some of the limits posed by fundamental material and process issues. An example of such issues is the interconnect delay, which in addition to limiting the attainable switching speed is also limiting chip size. The latter limitation can potentially be removed with optical solutions, such as microphotonics.

Vast majority of the integrated circuits manufactured and used today are built on single crystal silicon. The search for higher performance and lower cost for integrated circuits requires an increasing level of sophistication from the whole silicon manufacturing chain. The first stages of the silicon manufacturing chain are the purification of quartz sand into trichlorosilane gas, which is solidified as hyperpure polycrystalline silicon. The polycrystalline silicon is melted in special crucibles, and from this melt pulling of single-crystal silicon ingots is carried out. The crystal pulling is initiated with a small seed crystal, which is slowly pulled from the hot melt. Silicon solidifies on this seed crystal, atomic layer by atomic layer, exactly copying the crystal structure of the seed. Multi-staged wafering of these ingots results in thin, 0.5 to 0.7 mm thick slices, or wafers, cut from the single crystal ingot [3]. The actual devices, usually diodes or transistors, are built on mirror-polished single crystal silicon wafers using such techniques as optical lithography, oxidation, diffusion and ion implantation of dopants, epitaxy, and others.

Relentless pricing pressures and increasing sophistication of integrated circuits place ever-increasing demands on the starting materials. For the vast majority of semiconductor industry the starting material is a single crystal silicon wafer. Increasing demands placed on the silicon wafer give rise to novel approaches to the manufacturing chain in which quartz sand is transformed into integrated circuits. Throughout the silicon manufacturing chain there is a constant demand for reliable, precise and affordable measurement technology. The metrology demands range from bright light visual inspection, through

microscopy to some of the most complicated measurement devices industrially used today. Many of these challenges are best answered with optical metrology.

In order to fulfill the requirements posed by international trade the measurement systems used must be calibrated, often with very demanding uncertainty requirements. The calibrations are ultimately based on numeric definitions of physical quantities, which rely on international agreements on units and quantities. The availability of such well-defined quantities is guaranteed by international and national bodies responsible for the maintenance of standards, and traceable calibration chains to these standards [4]. Internationally maintained quantities are supplemented by national standards, maintained by national standards laboratories. National standards are required to shorten the calibration chains for the customers of the calibration services in industry and commerce. In addition, independent national standards are useful in gaining further verification for accuracy of the international standards. The semiconductor industry, like any other industry operating globally is increasingly required to provide traceable calibrations for their products. These requirements form a part of quality assurance systems, widely and increasingly required from suppliers in particular in high technology production.

The development of optical measurement technologies has placed unprecedented demands for metrological services of optical quantities. As the applications of optical technology are becoming increasingly important, the foreseeable demand for traceable calibrations of optical quantities is increasing. The ever-increasing importance of optical metrology is clearly apparent also in semiconductor industry. The Metrology Research Institute of the Helsinki University of Technology (HUT) was appointed as the National Standards laboratory for optical quantities in 1996.

The first part of the research work described in this thesis is closely related to the early stages of the National Standards laboratory, contributing to the development of the Finnish standards for spectrophotometric and radiometric quantities maintained at the HUT. This contribution has been significant. The experimentally verified model for spectral reflectance of a silicon photodiode, reported in Publication III has been widely utilized in radiometric research. The formulas for spectral reflectance and transmittance, derived directly from Fresnel formulas, as reported in Publication I, are the first straightforward and experimentally verified expressions reported for macroscopic layer thickness, for non-laser illumination. The results of the development of radiometry, in the form of detector-based realizations of radiometric and photometric quantities, rely heavily on the research and use of silicon photodiode detectors. Several radiometric applications rely heavily on linear detection systems. This requirement has been studied in the research reported in this thesis. A study on the absolute linearity of a silicon photodiode is reported in Publication V, and the results have been applied to comparative studies, reported in Publication IV. This work has provided results, which have been applied to development of a filter radiometer, reported in Publication VI.

The part of this work in which metrology is applied to semiconductor industry relates the development of silicon-based metrology to the measurement applications in which a piece of silicon crystal is the sample being studied. In particular, this research has

contributed to the sub-surface metrology of silicon wafers, prepared using fixed abrasive grinding, which as a manufacturing technique is rapidly gaining acceptance as a solution for reaching latest requirements placed on silicon wafers by the semiconductor industry. The comparative study reported in Publication VII is the first published study in which a comprehensive set of the available measurement techniques are directly compared. The advantages of advanced grinding techniques, together with the characterization methods developed for them, are discussed in Publication VIII.

This overview includes a short description of the silicon photodiode, and discussion on the use of silicon photodiodes in photometry and radiometry. The theory of reflection and transmission of light waves is considered, together with experimental results, for the purpose of spectrophotometric measurements. Characterization of silicon photodiodes is discussed in the context of detector-based radiometry. The structure and manufacturing process used to realize silicon photodiodes are described at a general level. The starting material of this manufacturing process, silicon wafer, and in particular the characterization of sub-surface damages in such wafers is discussed in more detail.

2. Silicon photodiodes

One important type of semiconductors, optoelectronic devices, covers the transformation of optical radiation into electronic signals, and vice versa. Optoelectronic devices can be divided on one hand to photo-generating devices such as LED's and lasers, and on the other hand to photo-sensing devices such as phototransistors, charge-coupling devices (CCDs), and photodiodes. Photodiodes are used for a huge variety of purposes ranging from telecommunications via optical interlocks to precision photometry. In this thesis, the silicon photodiode has been utilized for radiometric research. The structure and construction of a silicon photodiode, described below, explains the behavior of the device in spectrophotometry and radiometry. Manufacturing process of the photodiode is shortly described to illustrate the processes used in semiconductor industry to turn silicon wafers into various electronic devices.

The generalized structure of a silicon photodiode is presented in Figure 1. The depletion layer has been formed under the P-type layer on the left on the Figure 1a. In practice the depletion layer is much wider than the P-type layer, which is usually made as thin as possible.
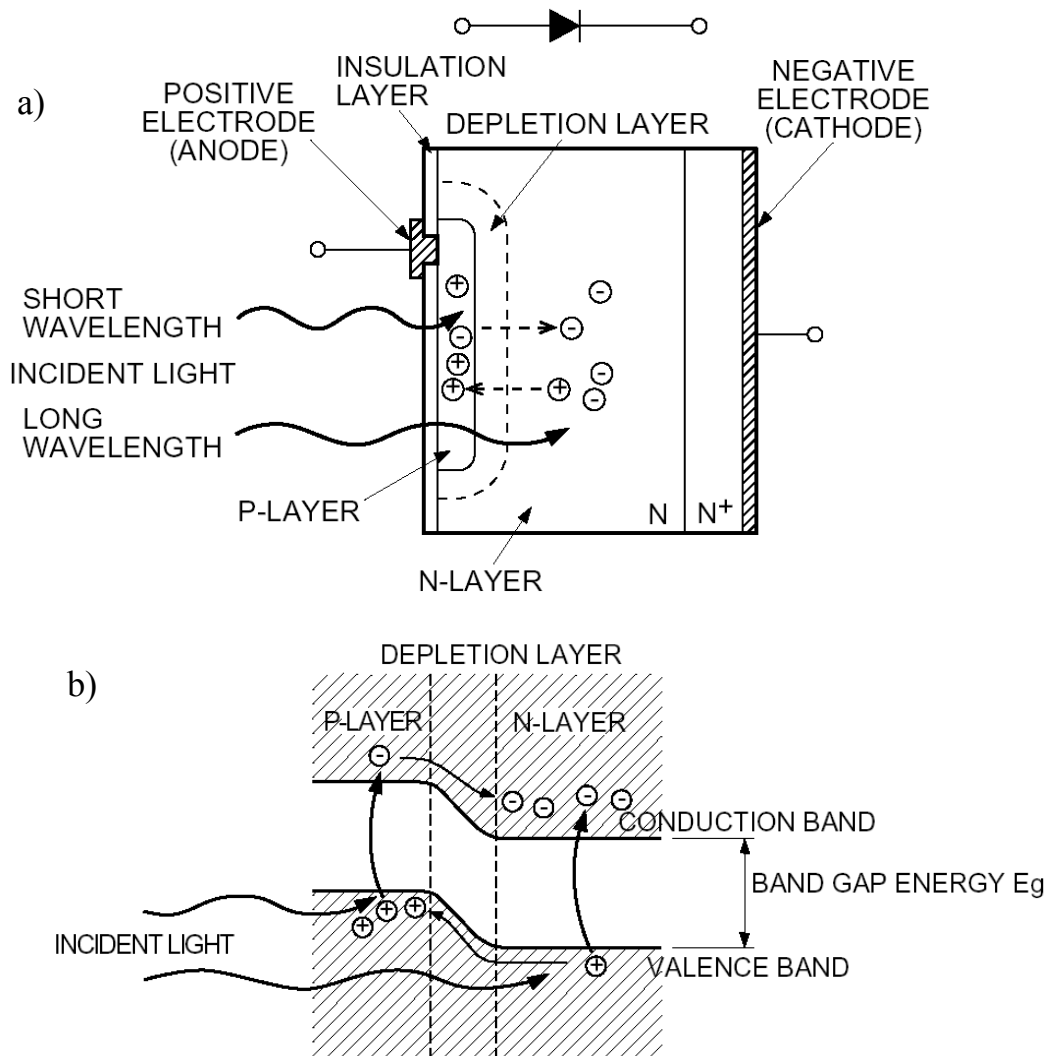
Figure 1　　Structural diagram of a silicon photodiode (a) and the energy level diagram of a P/N junction (b). In the Figure 1b the x-axis is the physical distance from the front surface, but the y-axis denotes energy levels for the current carriers. Absorbed photons generate electron-hole pairs, which are free to diffuse and if caught by the electric field in the depletion layer, be swept apart, generating current. From Ref. [5]

The photodiode is a device in which the electric field of the depletion layer of a p/n-junction is used to collect current carriers generated by photonic absorption. Photodiodes come in many flavors, usually tailored to a specific application. The spectral range in which a particular photodiode operates is fundamentally linked to the choice of semiconductor material used to manufacture the p/n-junction. The long wavelength limit of a photodiode is limited by the bandgap energy of the material used [6]. For wavelengths above the critical value λ_c, the photon energy is no longer sufficient to excite electrons to the conduction band and the material becomes transparent to those wavelengths. The low wavelength limit of a photodiode is caused by the reverse effect,

shortening absorption length, which limits the usability of a photodiode. This is due to the charge carriers being generated in the very surface of the semiconductor. For planar devices this is above the depletion zone, where, due to surface recombination the minority carriers have very short diffusion lengths – the carriers generated above the depletion zone are recombined before they can diffuse to the depletion zone. The short wavelength limit can also be influenced by the protective layers on top of the photodiode, which for short wavelengths can cause significant reflection and absorption losses.

Silicon is transparent to wavelengths above 1000 nm, and thus it is used for wavelengths up to near-infrared (NIR) only. For telecommunications usage at 1550 nm, other, more expensive materials such as Germanium or InGaAs must be used. The short wavelength cut-off of silicon photodiodes is not so well defined, but in the far UV, below 300nm, the quantum efficiency becomes increasingly problematic. For the environmentally important UVA and UVB wavelengths silicon photodiode is still a very good detection system.

The design of a photodiode involves several tradeoffs, one of the most basic decisions being the balancing act between responsivity, or quantum efficiency, the spectral effects of which were discussed above, and the frequency response. Very deep depletion layers offer the best internal quantum efficiencies, which for silicon photodiodes can approach 100% at 800-900 nm. Deep depletion layers translate also to long transit times and as a consequence, lowered bandwidths. The frequency response of a photodiode is also limited by the RC-product, in which the junction capacitance is defined by the depth and area of the depletion layer. Typically, the depletion width is matched to the required frequency response, both with respect to the capacitance and to the transit-time effects. Recently, novel designs have been proposed to overcome the optimization of the depletion width between quantum efficiency and transit time, through decoupling of the absorption length from the depletion width through novel design geometries. [Refs. 7, 8 and 9]

The p/n junction, or diode, forming a typical silicon photodiode for visual and near-infrared wavelengths is manufactured by planar diffusion of a group V element, in practice boron, into a n-type substrate silicon wafer. This takes place in a high temperature furnace, where, at a temperature of some 1000-1200 C, boron diffuses in the silicon lattice. Diffusion takes place from the wafer surface down into the wafer, creating a shallow region, which is effectively p-doped. While the depth of the diffused p-type layer is typically less than 1 μm, the p/n junction formed below the diffused p-layer creates a depletion region, which can reach several microns. The design of the photodiode aims at increasing the proportion of the photons of interest, which are absorbed in the depletion region. In the depleted region the built-in electric field due to the p/n junction sweeps the generated current carriers to anode and cathode parts of the diode, preventing recombination and thus increasing the responsivity of the device. Absorption within depletion layers are enhanced through combination of thin diffused p-layer, to minimize absorption in the p-layer, high resistivity n-type substrate wafer in which the low dopant concentration yields wide depletion regions, and, in some cases, spectrally weighting coatings. In many cases an external voltage bias is used to widen the depletion region. If the external reverse bias is enough to accelerate the current carriers

up to ionization energies, multiplication of current carriers takes place. This multiplication creates an avalanche of current carriers, and gives rise to internal current gain. Such a device is called an avalanche photodiode (APD).

Prior to the diffusion, the wafer has been patterned using optical lithography. In lithography a photosensitive layer, photoresist, is first spun on top of the wafer. It is then illuminated with a light beam using a master mask, in order to define the required geometries. The developed resist is subsequently used to define areas to be masked using oxide or nitride layers. The diffusion of boron is effectively masked using a thin silicon dioxide film. After the creation of the p/n junction with the boron diffusion, the backside of the wafer is diffused with some group VI element (antimony, arsenic or phosphorus) in order to lower the series resistance and to improve the ohmic contact at the back of the diode. An additional lithography step is required to define the bond pad locations required for contacting of the photodiode. The actual bond pad contacts for the anode and cathode are usually sputtered with aluminum. A thermal oxide grown on top of the p-type planar diffusion creates a quartz, or SiO_2, window required for UV measurements. Alternatively, a resin window can be used if UV-suppression is required.

The quantum efficiency of a silicon photodiode can be improved with a design in which the depletion layer width is greatly enhanced. This can be combined with a very thin p-diffusion layer for enhanced UV-responsivity. The widening of the depletion layer is typically achieved by using a high-quality n/N+ epitaxial wafer as the starting material. In this type of wafer a high resistivity, low dopant concentration, n-type layer is epitaxially deposited on top of a low resistivity, high dopant concentration, n+ type starting wafer. Use of an epitaxial wafer provides an extremely uniform, nearly ideal silicon layer for the active device. Such a wafer has a very high resistivity top layer, enabling wide depletion layers. A further development in which the widening of the depletion layer is carried even further results in the PIN photodiode (P-type - Intrinsic - N-type), which offers fast response times, especially if reverse-biased. The tradeoffs discussed earlier do, however, pose limits to the manipulation of the frequency response. The APD and PIN photodiodes, together with Schottky-photodiode are the preferred designs for very fast applications, such as telecommunications, for which the frequency limitations are most critical.

3. Use of silicon photodiodes in radiometry and spectrophotometry

Radiometry is defined as the science and technology of measurement of electromagnetic energy [10]. One of the most important applications of optical radiometry is the realization of the SI-unit candela, the unit for luminous intensity. This quantity is linked to the corresponding radiometric quantity, radiant intensity, through a weighting function. This weighting function, known as the $V(\lambda)$-function is defined to describe the spectral responsivity of the human eye [11]. The most reliable realizations of candela, that is, those with the lowest uncertainties, are based on filter radiometers built around silicon photodiodes [12, 13, 14].

The realization of radiant power scales can be based either on primary sources or primary detectors. The source-based realizations of the radiant power scales are, and have always been associated with black body radiators. The radiant power emitted through a small opening in a cavity can be calculated with the Planck's radiation law. The only requirements are that the cavity is in thermal equilibrium and that the temperature of the cavity is separately measured. In order to reach useful intensities in the optical wavelengths the black body radiator must have a very high cavity temperature, which poses practical difficulties with the available materials and the complexity of the instrumentation, required for such a device.

The performance of the detector-based radiant power scales, based on calorimetric substitution, depends heavily on the temperature of the absorption cavity. The development of cryogenic radiometers has improved the attainable uncertainty for detector-based radiometry in the past two decades. This has led to increasing reliance on detector-based realizations for spectral irradiance and radiant power scales. At the moment whenever low uncertainties are required in the realization of radiometric power scales for wavelengths near the visible spectrum the scale is based on cryogenic radiometers [15, 16, 17]. The detectors used to transfer these primary realizations of radiant power are typically high-quality silicon photodiodes.

4. Reflection and transmission of light waves

Whenever the propagation of electromagnetic radiation is disturbed by discontinuities in the transmitting media the energy of the radiation is divided in two parts. These parts are the energy of the wave reflected from the discontinuity, or surface between two uniform media, and the energy transmitted through the surface. The reflection and refraction of light at a surface between two media is governed by the law of reflection and the Snell's law for the direction of the beam propagation, by the Fresnel complex amplitude coefficients[18] for the amplitude of the propagating waves.

Simple surfaces are rarely encountered on macroscopic scale and for several macroscopic samples the reflected and transmitted waves are therefore combinations of multiple

internal reflections between the various surfaces of the sample. The simple case in which two parallel surfaces limit a uniform sample is described in Figure 4.
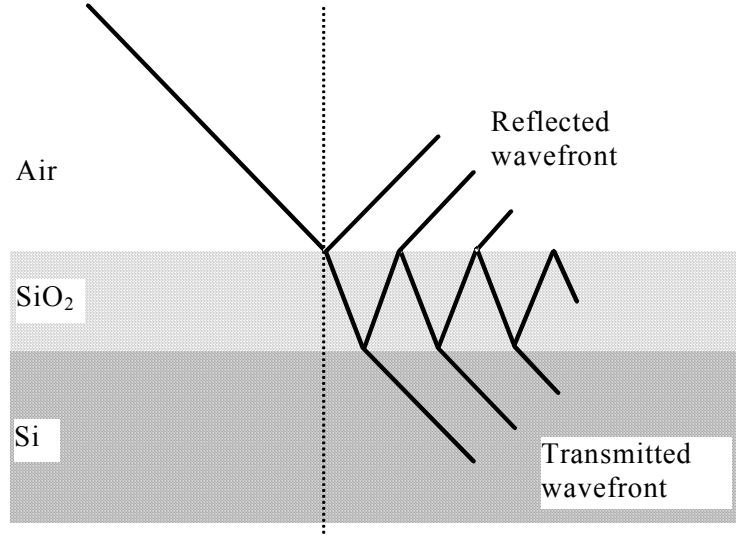

Figure 2   Internal reflections of a parallel light beam in a macroscopic sample (silicon photodiode). Both the reflected and the transmitted beam consist of an infinite sum of component waves.

Depending on the coherence length of the light beam, the interference of the component waves of the wavefronts drawn in Figure 2 will have different effects on the intensity of the reflected or transmitted waves. For a silicon photodiode with a sub-wavelength thick quartz or resin window, the optical path difference of the reflected beams is within coherence length of broadband illumination, and the basic reflection and transmission equations [18] apply:

$$\bar{r} = r_{12} + \frac{t_{12}t_{21}\bar{r}_{23}\exp(-2i\beta)}{1 + r_{12}\bar{r}_{23}\exp(-2i\beta)} \quad , \tag{1}$$

where r_{mn} denotes Fresnel reflection coefficient for the interface mn, t_{mn} denotes Fresnel transmission coefficient for the interface mn, and β denotes the phase difference between two subsequent wavefronts exiting the front surface of the window material.

The spectrophotometric quantities of a sample due to the interreflections inside the material layers depend not only on the wavelength dependent optical properties of the media, but also on the thickness of the sample, angle of incidence and the spectral and angular distribution of the incoming beam of light. The reflection and transmission for samples in which the optical path difference exceeds the coherence length of the incoming radiation require some changes to the basic Fresnel's formulas presented above. The appropriate equations, based on Fresnel's formulas, that describe these processes have been derived in separate and largely dissimilar manner both for transmittance [19]

and reflectance [20]. The straightforward derivation presented in Publication I is identical for both transmittance and reflectance.

5. Spectrophotometric measurements

One of the key components in the development of optical metrology has been the realization of reference spectrometers for spectral transmittance and reflectance measurements. The macroscopic transmittance and reflectance of light can be divided into specular, also called regular, and diffuse parts. For the smooth, polished surfaces of optical components like filters and mirrors, the regular component dominates both in reflectance and transmittance. Diffuse reflectance is an important quantity in various fields of colorimetry, including paper industry and the study of imperfections in surfaces dominated by the specular reflectance. In the development of national standards for spectrophotometric quantities at the Helsinki University of Technology, HUT, a path was chosen in which the standards for regular components were to be developed first. Accordingly, the reference spectrophotometer for measurement of regular transmittance was designed and constructed before the development of a reference spectrometer for diffuse reflectance.

The spectrophotometer for measurements of regular transmittance was from the outset designed for automated measurements enabling routine calibrations to be carried out at high accuracy level [21,22]. The components of measurement uncertainty have been identified, analyzed and minimized. The spectrophotometer has proved to reliably yield high performance, and calibration of filters both for calibration services and for development of radiometry and photometry has worked remarkably well. The wavelength range of the instrument has been expanded into UV and the near infrared regions, while maintaining the low uncertainties reached in the visible region. An accessory for measurements of specular reflectance has been successfully implemented [23]. An example of reflectance measurement results close to the Brewster's angle of the sample is presented in Figure 3. The theoretical calculation presented in the figure includes no free parameters for fitting, and thus the excellent agreement between the experimental and theoretical results verifies the formulas used.
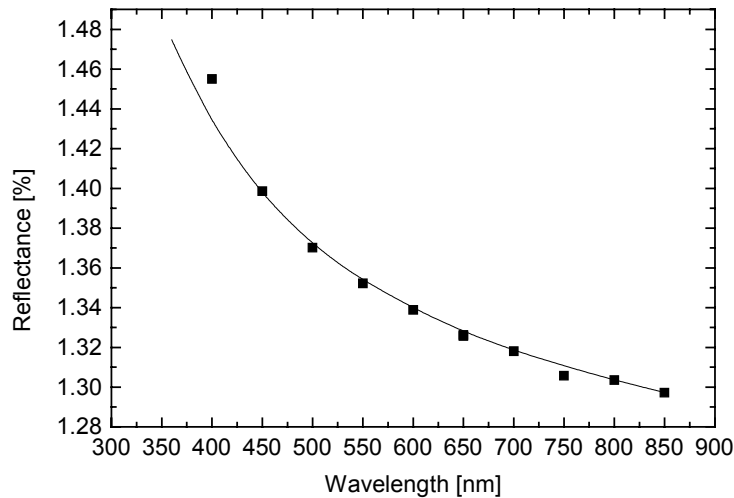
Figure 3   Result of a test measurement carried out with a 3-mm thick sample of UV-grade synthetic fused silica. The measurement beam was linearly polarized in the plane of reflection (p-polarization), and the angle of incidence was 45 degrees. The continuous line denotes the theoretical reflectance of the sample calculated according to the formulas presented in Publication I.

The low uncertainties quoted for the instrument have been verified in international intercomparisons and test measurements carried out for samples for which the relevant optical properties are known. The design, construction and analysis of the uncertainties reached with the reference spectrophotometer at HUT is described in Publication II, together with some of the results of the intercomparisons and test measurements

6. Characterization of silicon photodiodes

The silicon photodiode benefits from the nearly ideal internal quantum efficiency over a wide range of incoming signal intensities. On the other hand, there are several mechanisms, which limit the current generation at high signal intensities. As the generated current increases, the electrical circuit created around the silicon photodiode begins to be affected by the voltages caused by the various unavoidable resistance and the current generated. The low series resistance typical to modern, high quality silicon photodiodes allows signal currents up to some 1 mA to be measured before the voltage drop over the ideally unbiased photodiode begins to deteriorate the performance of the photodiode. The sensing circuit also affects the system linearity. Incident light on the photodiode's active area produces a photocurrent which is usually measured by the amount of voltage drop across an external resistor, which for high sensitivity is required

11

to have high resistance, up to tens of MΩ. Thus the external circuit can also create unwanted bias voltages over the photodiode, unless the circuits are carefully optimized.

In addition, there are mechanisms associated with the amount of current generated in the given volume of active detector. To maintain the ideal quantum efficiency, the incoming photon must be absorbed in the depletion layer, creating an electron-hole pair. Increasing signal current inevitably leads to higher carrier concentrations in the doped regions of the diode. In the surface P-layer, the increasing free carrier absorption poses one volume-based limit to quantum efficiency at high signal currents. As long as the photo-generated current density is well below the carrier density in the active area, these effects do not materially affect the generated photocurrent [24].
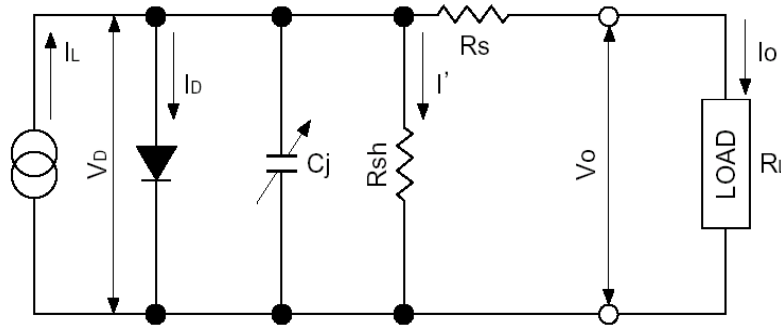

Figure 4   The equivalent circuit of a photodiode. In the figure, the following abbreviations are used: I_L, current generated by the incident light, I_D, diode current, C_j, junction capacitance, R_{sh}, shunt resistance, R_s, series resistance, I' shunt resistance current, V_D, voltage across the diode, I_o, output current, V_o, output voltage.

For precision radiometry, the most useful signal obtainable from a photodiode is the short circuit current I_{SC}, which is reached for $R_L = 0$ and $V_o = 0$. Using the symbols of Fig. 4, I_{SC} can be written as

$$I_{SC} = I_L - I_S \left(\exp \frac{e \cdot (I_{SC} \cdot R_S)}{kT} - 1 \right) - \frac{I_{SC} \cdot R_S}{R_{sh}} - ...., \tag{2}$$

where the higher order terms have been omitted. In high-quality photodiodes, measured using optimized circuitry, the value of R_s is in the order of few ohms, whereas R_{sh} is some 10^7 to 10^{11} ohms, and thus the second and third terms become negligible over a wide range of generated photocurrent. Thus the advantage of using I_{SC} is realized as the measured signal I_o is reduced to the generated photocurrent, which in turn is directly proportional to the photon flux to be measured.

The exact relationship between small-signal behavior and the operation of the photodiode, or any photovoltaic device, at varying signal currents is defined as the linearity of the detector. This property has been verified to vary for different types of devices, as reported in Refs. 25 and 26. An independent characterization of this quantity for high quality silicon photodiodes is reported in Publications IV and V, the former investigating the relative linearity behavior of several high-quality silicon photodiode types over several decades of signal intensity. Publication V investigates the absolute linearity behavior of a silicon photodiode chosen as the benchmark detector in the relative linearity study.

The linearity characterization measurements are based on comparison between the generated photocurrent I_{SC} and an illumination level, which can be varied in controlled fashion. In this work, it was decided to limit the investigations to DC signals, as the AC signals are rare in precision measurements needed in radiometry.

7. Silicon photodiode and detector-based radiometry

Transfer standards are needed in order to transfer the high accuracy in optical power measurements reached with the cryogenic absolute radiometer to everyday calibrations. High-quality silicon photodiodes have several desirable features for such a transfer detector, including low cost, high responsivity, low thermal coefficient, and low spatial nonuniformity. The spectral responsivity $R(\lambda)$ of a silicon photodiode can be written as

$$R(\lambda) = [1 - \rho(\lambda)]\varepsilon(\lambda)\frac{e\lambda}{hc}, \tag{3}$$

where $\rho(\lambda)$ is the spectral reflectance of the photodiode, $\varepsilon(\lambda)$ is the internal quantum efficiency of the photodiode, and e, h, c are fundamental constants. Thus, the spectral behavior is defined by the spectral functions $\rho(\lambda)$ and $\varepsilon(\lambda)$ in equation (3).

Silicon photodiodes reflect a rather large proportion of the incident light, which obviously has a detrimental effect on the external quantum efficiency. As accurate prediction of the reflectance is difficult, there is a need for similar photodetectors with lower reflectance. This requirement arises for instance in precision radiometry, for transfer standard use. This requirement has been fulfilled with the development of the trap detector [27], a construction in which three silicon photodiodes are arranged to absorb the reflected light in a series of reflections between the component photodiodes. The residual reflection is directed out of the device, but it is two decades lower in magnitude, compared to the reflection of a single photodiode. The advantages and applications of such devices are described in Refs. [28,29].

For the visible wavelengths, to a very good approximation, the absorption of a photon in a silicon photodiode creates one electron-hole pair. For absorbed photons the behavior is

thus close to ideal photoelectric conversion, or 100% internal quantum efficiency. The deviations of silicon photodiodes from this ideal are well understood, and they can be accurately modeled [30, 31]. The shape of the spectral responsivity curve is a product of the linearly rising responsivity of a ideal photoelectric conversion, and the absorption curve, which starts to fall somewhere between 700 and 900nm, depending on the width of the active region.

In Figure 5, the calculated spectral responsivity of a simplified model of a single silicon photodiode, and reflection trap detector based on the same photodiodes, are presented. The calculation is based on the material properties of silicon only, except for the thickness of the quartz window, and the width of the depletion layer. The thickness of the quartz window has an effect on the spectral reflectance of the photodiode, and the width of the depletion layer defines the absorptance of the photons entering the silicon material. The width of the depletion layer, 10 μm, has been calculated from the specified terminal capacitance of the particular type of photodiode, Hamamatsu S1227. The depletion layer has been calculated assuming that the capacitance is a straightforward function of the depletion layer thickness and area only. The contribution of the current carrier generation taking place within diffusion length of the depletion layer has been ignored, and thus the calculation underestimates the true responsivity. In more detailed calculation models the contribution due to current carrier diffusion is modeled with fitted parameters [30, 31].

For the rough estimate depicted in Figure 5 the window thickness, 28nm, is the only parameter that has been separately measured from the photodiode [Publication III]. Even this very rough approximation shows that, in the visible wavelengths, by far the largest deviation from the ideal photoelectric conversion is due to the reflectance of the diode front surface. Trap detector, for which the reflection losses are two magnitudes lower than those for a single photodiode, offers external quantum efficiency very close to ideal photoelectric conversion. Even ignoring current carriers diffusing from below the depletion zone the calculated responsivity of the trap detector is practically equal to the ideal photoconversion, up to 750 nm.
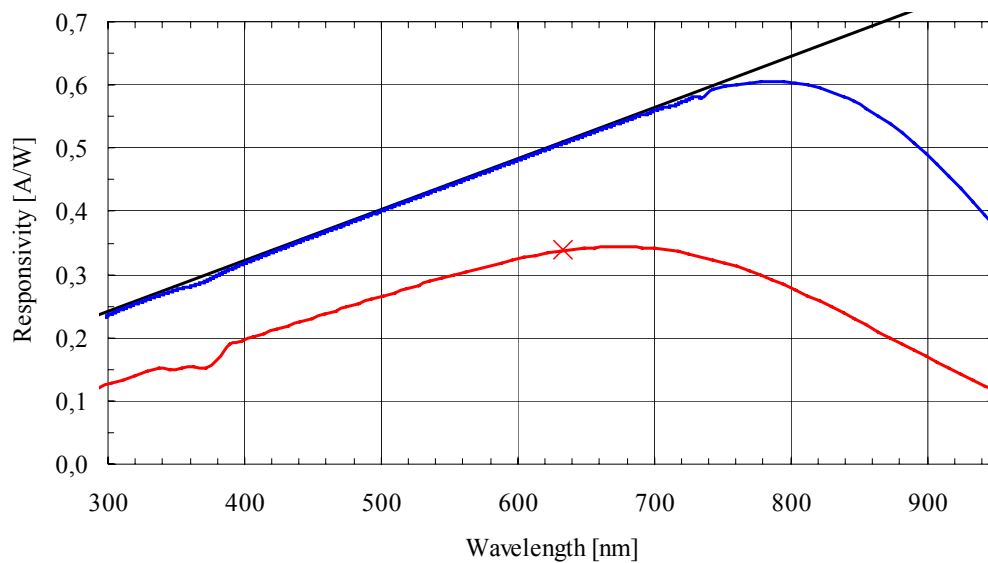
Figure 5 Calculated spectral responsivity of a high-quality silicon photodiode of a type used in spectrophotometric and radiometric measurements. The red line denotes the calculated responsivity of a single photodiode for known material parameters of silicon; the cross denotes supplier specification value for single photodiode responsivity at the He-Ne laser wavelength of 633 nm. The blue line represents corresponding calculation for a reflection trap detector and the black line denotes the responsivity of an ideal photoelectric conversion, with 100% quantum efficiency.

The residual reflection out of the trap detector is very small in the visible wavelengths, but increases rapidly deep in the UV. For the requirements of precision metrology, the reflectance of a trap detector can be accurately modeled with a simple model, in which a silicon photodiode is described as a substrate of pure silicon, on top of which lays a thin layer of silica (SiO_2). The validity of this model has been verified by a series of reflectance measurements, which have been compared with reflectance calculated with the help of Fresnel's equations and the simple model described above. This verification is described in more detail in Publication III.

In visible wavelengths the model for the reflectance of the silicon photodiode is highly accurate, yet it is of relatively greater importance for applications at the UV wavelengths. Particularly important are the environmentally important wavelengths in the UV-B region. In this wavelength band, the trap detector based on silicon photodiodes gives rise to several interesting applications, such as reported in Ref. 32. These applications benefit from the accurate prediction of the reflection losses enabled by the model presented in Publication III. In Ref. 33 the spectral responsivity model of silicon photodiode trap detector has been extended to 260 –950 nm, resulting in agreement between the modeled and measured responsivity at the level of 0.8% (k=2). This was reached by combining accurate reflectance models with physical model for impact-ionization induced internal

gain for photon energies above the direct bandgap of silicon, 3.1 eV, corresponding to wavelengths below 400nm.

Utilizing a cryogenic absolute radiometer as the primary standard for optical power at certain laser wavelengths, a well-characterized trap detector as a transfer detector, an accurately measured interference filter, and a precision aperture, a filter radiometer with several desirable properties can be constructed. One of the main sources of uncertainty in filter radiometers is the effect of interreflections between the filter and the photodetector, which is usually a photodiode. When substituting a trap detector for the single photodiode, the interreflections are greatly diminished. In addition, by accurately determining the reflectance of both the trap detector and of the interference filter even the residual interreflection can be modeled, and a correction calculated. With this method the effect of interreflections can be eliminated to such a degree that it is possible to change the interference filter without compromising the measurement accuracy of the radiometer. A schematic diagram of such a filter radiometer utilizing a trap detector is presented in Figure 6.
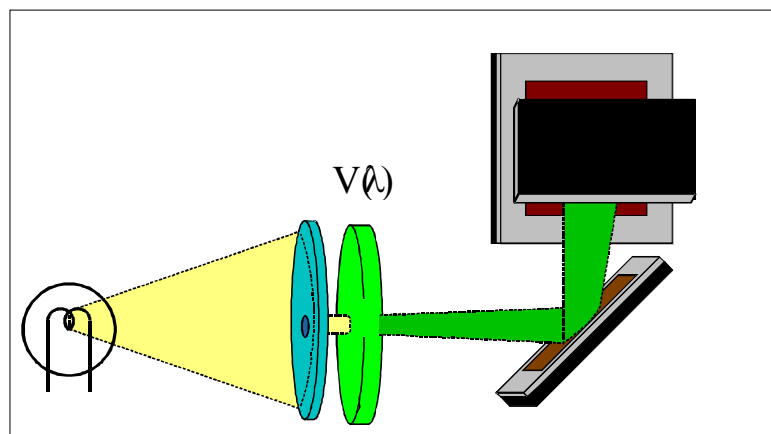

Figure 6   The principle of a filter radiometer combined with a trap detector. A lamp is used as the light source. The field of view of the radiometer is defined by the precision aperture (blue), after which the bandpass filter is used to define the part of the spectrum to be measured. The trap detector, constructed from three silicon photodiodes is used to convert the incoming light into a current signal.

As the effects of interreflections are minimized, a single, carefully characterized trap detector, a temperature-controlled housing, an aperture, and a set of interference filters can constitute a detector-based realization of the spectral irradiance scale. This system also allows a lamp to be fully characterized with a single alignment of the filter radiometer, as the filters are easily interchangeable. Based on the measurements carried out with the filter radiometer, the spectral radiance of the lamp can be calculated with relatively straightforward fitting of the Planck's law, corrected for the emissivity of the filament. The expanded (k=2) uncertainty for the HUT spectral irradiance scale varies

between 3.1% to 1.0% from 290 nm to 900 nm, respectively [34]. The extension of this scale down to UV wavelengths has allowed detector calibrations at the environmentally important wavelengths around 312 nm with very low uncertainties. The calculation procedure used in the derivation of the scale is described in detail in Refs. [35, 36]. The same design is also used as a realization of the luminous intensity scale, by replacing the interference filter with a separately characterized V(λ) filter. This type of filter radiometer is studied in Publication VI.

8. Characterization of sub-surface damages in silicon wafers

Many applications of optical metrology are well established in the semiconductor industry, such as optical microscopy and surface laser scanning. Some new measurement applications, arising from changes in the silicon manufacturing chain are still being defined and tested. One such application is the characterization of sub-surface damage due to abrasive machining of semiconductor materials. In semiconductor industry such sub-surface damage has traditionally been characterized through combinations of iterative layer removal, visual inspection, optical microscopy and X-ray diffraction. For sub-surface inspection of fabricated devices optical microscopy has recently been enhanced, reaching below the half-wavelength criteria in spatial resolution [37].

Figure 7 depicts the results of a removal test in which a single grinding-induced crack was iteratively removed, with SEM inspection between removal steps. The cracking was performed with a single pyramid-shaped diamond at the scratching speeds of 30m/s. Unfortunately, iterative methods are, by nature, time-consuming, costly, and thus unsuitable either for continuous process control or for statistical analysis of generated sub-surface damage. They do, however, provide a vital link between the wafer manufacturing process and the development of advanced process control methods.

Another example of inspection results, based on iterative layer removal using chemical-mechanical polishing (CMP) is presented in Figure 8. The radial, twisted grooves imaged are due to the geometry of the rotational grinding. The fact that the most severe damage is observed at the edges is due to the width of the cut, which for rotational grinding is much wider at the edge than at the center. The damage identification was based on local texture variation caused by caustic polishing slurry on damaged lattice-points. Detection of the local texture was implemented with the differential contrast (DIC) channel of a laser scanner of the type Surfscan SP-1 by KLA-Tencor, Inc, San Jose, CA, USA. This inspection is similar to that used for prime silicon wafer inspection before shipping wafers to IC manufacturers, and thus the inspection criteria is that required in the semiconductor industry.

17

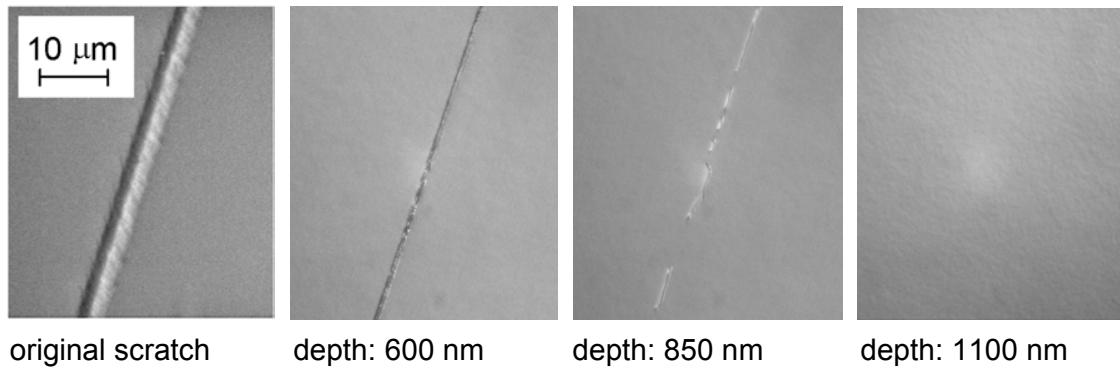original scratch   depth: 600 nm   depth: 850 nm   depth: 1100 nm

Figure 7   The propagation depth of a linear scratch in single crystal silicon. The SEM images have been taken at the same location at various stages of layer removal. The depth indicated below each image refers to the total thickness of the layers removed prior to imaging.
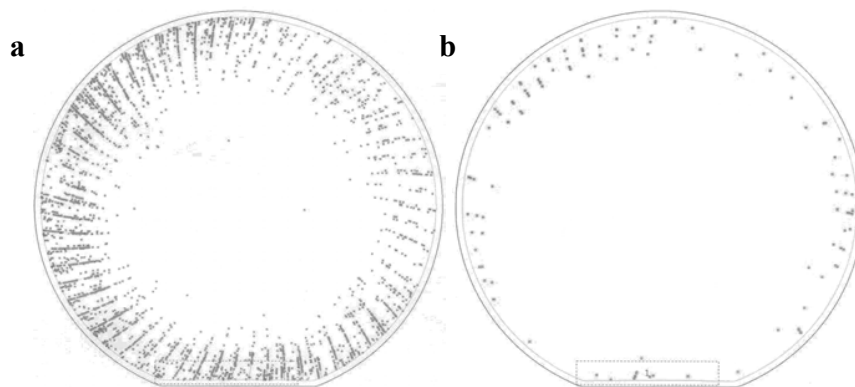

Figure 8   Removal of the grinding damage in CMP. These graphs represent scanning results of KLA-Tencor SP-1 surface inspection machine. The ductile ground wafer sample has been iteratively polished for increasing layer removal. The graphs a and b represent measurements after one and two polishing iterations, respectively.

One of the most studied forms of sub-surface damage is the damage due to ion implantation. The crystal damage due to ion implantation can be characterized with such methods as optical reflectance, ellipsometry and photothermal analysis [38,39,40]. These methods, however, typically require mirror-polished surfaces. Introduction of fixed abrasive grinding to the wafer manufacturing has introduced new requirements for damage characterization, also for non-mirror polished silicon surfaces. Advanced grinding technology is being rapidly applied to state-of-the-art wafer manufacturing processes, providing extremely low thickness variations combined with ductile mode grinding with shallow layers of damaged crystal. Standard CMP process is used for polishing these surfaces and revealing the undisturbed crystal for circuit manufacture. In order to ensure both the absolutely defect-free front surface of silicon wafers, required by the ever more sophisticated integrated devices, and competitiveness in the ever more

challenging market competition, accurate analysis methods must be used for process optimization. Advances in grinding technology and analysis of the sub-surface damage levels attained in ductile grinding of silicon surfaces are presented in Publication VIII. A qualitative description of the sub-surface damage due to rotational grinding of silicon wafers is presented in Figure 9.
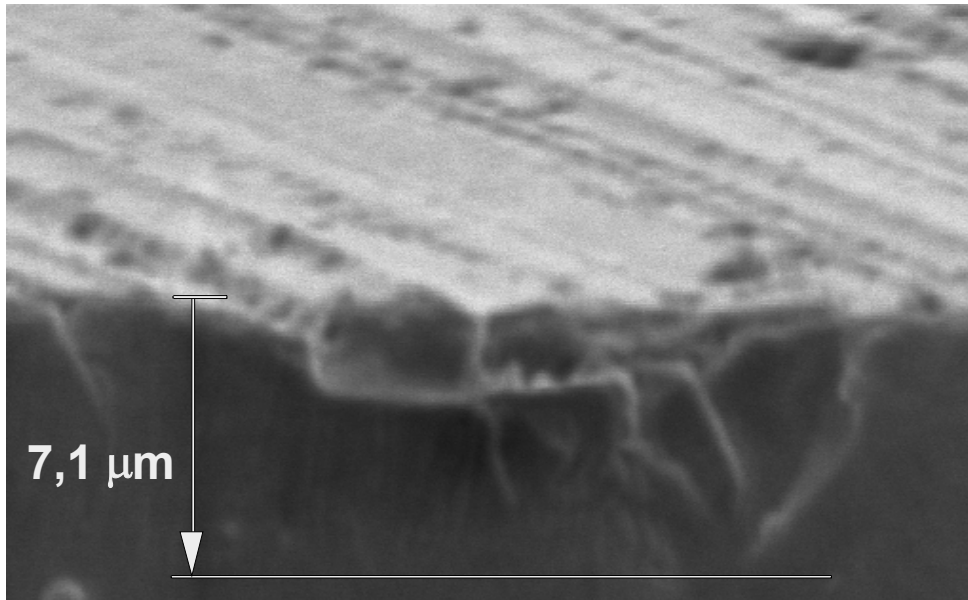

Figure 9 SEM image of a cleaved silicon wafer surface after rotational grinding. The grinding was carried out mostly in the brittle mode. Crack depth can be approximated from the image.

Variety of methods has been proposed for nondestructive characterization of the sub-surface damages in semiconductor material, primarily silicon wafers processed to varying degree. In Refs. [41] and [42] the traditional lapping techniques are compared with fixed abrasive grinding using a number of characterization methods. Truly workable single solution to the characterization problem has not been found. It has turned out that in order to understand both the nature and extent of the sub-surface damage several investigations must be carried out. Also, some methods are inherently more suited to specific surface conditions and to particular extent of damage, which limits the possibilities of using the same methods throughout the long manufacturing chain. Some of the methods, such as those presented in Refs. 43, 44 and 45, which yield most accurate data, are not applicable to production environment requiring rapid, non-destructive and preferably mapping analysis of wafers while they are being processed.

Direct comparison of a number of potential analysis methods was carried out. In this experiment a number of 200mm silicon wafers were ground using several grinding wheels and a G&N Nanogrinder automated grinding machine. A fixed set of machining parameters was used for wafer planarization using all the grinding wheels included in the

test. The parameters varied were the spindle rotation speed, or the tangential velocity of the wheel (30-90 m/s), infeed of the wheel (3-9 um/min), and wafer rotation (100 / 200 rpm). Repeatability of the ground silicon surfaces was determined with wafer strain-induced deformation measurements, roughness analysis and visual inspection. Based on the good repeatability of the machined surface properties it was deemed sufficient to repeat each test 5 times. With 5 different fine grinding wheels and 18 machining parameter combinations this resulted in a sample set of 450 wafers. Potential methods for determining the sub-surface damage induced to silicon wafers during grinding were compared using these ground sample wafers. This direct comparison of seven potential measurement methods is presented in Publication VII. One of these methods is based on the work of spectrophotometry carried out at the HUT. Laser-based optical scattering has recently been proposed as a solution to characterization of sub-surface damage in silicon machined wafers [46]. The results reported in this thesis indicate that spectroscopic application provides potential for gaining insight to the in-depth distribution of the lattice damage.

9. Conclusions

True understanding of any measurement result requires detailed study and characterization of the system used to produce the said result.

One challenging field for spectrophotometric measurements has been the environmentally and medically important gauging of optical power in the UV wavelengths. Significant improvements have been achieved in reducing uncertainties due to the measurements, required to quantify the risks due to exposure to UV wavelengths.

In this thesis, the spectrophotometric and radiometric research done at HUT is presented. This research is focused on detector-based realizations of the units of spectral radiance, spectral irradiance and luminous intensity. These realizations rely heavily on trap detectors. Trap detectors are constructed from silicon photodiodes, and this thesis outlines the central role of this device in the optical branch of research in metrology. Physical principles behind the operation of silicon photodiodes are discussed. This thesis outlines experimentally verified models, which enhance the utility of silicon photodiodes for demanding spectrophotometric and radiometric measurements. This enhancement is achieved through well-defined corrections based on simple yet effective models.

The accurate characterization methods used to enable successful use of silicon photodiodes in precision metrology are presented. The research covered in this thesis has formed a part of the reliable, detector-based realizations of optical quantities, maintained at the Metrology Research Institute (MRI) as national standards. The experimentally verified formulas for spectral reflectance and transmittance have been widely utilized to reduce the uncertainties of spectrophotometric applications of silicon photodiodes. The radiometric research carried out at MRI has significantly contributed to the improvements in optical measurement technology, especially in UV wavelengths.

The measurement challenge posed by novel methods in abrasive machining of silicon wafers for semiconductor industry is outlined. Various methods, based on a number of different physical principles, have been proposed for sub-surface damage characterization of machined silicon wafers. Analysis of these various methods, carried out in the course of the work described in this thesis, reveals that while the physical properties observed with the varying techniques vary, the processes which deform the properties of the lattice are closely linked. The reported analysis is based on a direct comparison of several methods, varying in the physical observable quantities. Further research is encouraged to study the development potential of the methods presented. Deeper understanding of the mechanisms of lattice perturbation in ductile machining of brittle materials also greatly benefits the development of those machining techniques and modeling thereof.

Summary of publications

High-Accuracy Measurement of Specular Spectral Reflectance and Transmittance
Analytica Chimica Acta **380**, 317-325 (1999).

The realization of spectrophotometric quantities at the Helsinki University of Technology (HUT) is based on our reference spectrometer. The reference spectrometer is a high-accuracy instrument developed for measuring spectral specular transmittance and reflectance in a wavelength range extending from ultraviolet to near-infrared. The relative uncertainty estimates for transmittance measurements of neutral density filters are in the range of 0.05%. For spectral reflectance the estimated relative uncertainties are between 0.14 and 0.34% depending on the sample reflectance and the measurement geometry.

We have derived and verified equations that enable both the reflectance and transmittance of various samples to be predicted. Utilizing these equations, the reflectance and transmittance can be accurately calculated for samples with known refractive index. For precise calculations, the characteristics of the measurement beam must be taken into account.

Precision spectrometer for measurement of specular reflectance
Review of Scientific Instruments **73**, 2237-2242 (2002).

Reference spectrometer has been modified for measuring specular reflectance in the wavelength range of 300 to 850 nm. The whole instrument is based on a diffraction-grating monochromator, reflecting optics, sample control mechanics and linear detection systems. Relative standard uncertainties between 0.14 and 0.32% have been estimated for the reflectance measurements. For spectral reflectance between 1.5 and 15%, the results of test measurements confirm that for all geometries the relative deviations are below 0.36%. A set of UV-interference filters have been measured in the UVB wavelength range, and the results are used as a part of UV-filter radiometer characterization.

Spectral reflectance of silicon photodiodes
Applied Optics **37**, 729-732 (1998).

A precision spectrometer was used to measure the spectral reflectance of a silicon photodiode over the wavelength range from 250 to 850 nm. The results were compared with corresponding values predicted by a model based on thin-film Fresnel formulas and the known refractive indices of silicon and silicon dioxide. The good agreement at the level of 2×10^{-3} in the visible wavelength range verifies that the reflection model can be used for accurate extrapolation of the spectral reflectance and responsivity of silicon photodiode devices. In addition, characterization of the photodiode reflectance in the ultraviolet region improves the accuracy of the spectral irradiance measurements when filter radiometers based on trap detectors are used.

Measurement of absolute linearity of photodetectors with a diode laser.
Measurement Science and Technology **10**, 1075-1078 (1999).

An automated instrument based on the beam addition technique has been developed for measurement of the linearity of photodetectors. The system is designed for absolute characterization of a transfer standard photodetector, against which the linearity of other detectors can be measured. The measurement set-up has been made as simple as possible. A diode laser at 633 nm is used as the light source due to the good stability and high power output available with the device. Two measurement beams of 0.9mm diameter are aligned to intercept on the photodetector. As an example, a silicon photodiode of the type S1227 has been studied and found out to be linear within $3 \cdot 10^{-5}$ up to 7 mW of optical power.

Nonlinearity measurements of silicon photodetectors
Applied Optics **37**, 2716-2722 (1998).

Nonlinearities of the responsivity of various types of silicon photodetectors have been studied. These detectors are based on photodiodes with two sizes of the active area (10 x 10 mm^2 and 18 x 18 mm^2). The detector configurations investigated include single photodiodes, two reflection trap detectors, and a transmission trap detector. For all devices, the measured nonlinearity was less than 2 x 10^{-4} for photocurrents up to 200 mA. The diameter of the measurement beam was found to have an effect on the nonlinearity. The measured nonlinearity of the trap detectors depends on the polarization state of the incident beam. The responsivity of the photodetectors consisting of the large-area photodiodes reached saturation at higher photocurrent values compared with the devices based on the photodiodes with smaller active area.

Filter radiometry based on direct utilisation of trap detectors
Metrologia **35**, 255-259 (1998).

A new design of a filter radiometer based on a trap detector, a set of temperature-controlled filters, and a precision aperture is described. This filter radiometer can be used to realise high-accuracy scales for illuminance, luminous intensity, and spectral irradiance. The new filter radiometer is an improved version of our earlier designs. It has been improved in such a way that the filter can be easily and reliably changed. This makes it more suitable for spectral irradiance measurements, where lamps usually have to be measured at several wavelengths. The results of the characterisation of the filter radiometer equipped with a $V(\lambda)$ filter using two different methods are presented. The results are in agreement at the level of 0.3 %.

Rotational grinding of silicon wafers – Subsurface damage inspection
Materials Science and Engineering B **107**, 321-331(2004).

Industrial practise in wafer manufacturing indicates that there is not one agreed method available to acquire a conclusive picture of the sub-surface damage, defined as structural

inhomogeneities of the crystal lattice. Therefore, various methods have been studied and compared for measurement of the sub-surface damage introduced to single crystal silicon wafers during rotational grinding process. Several probing techniques were used to analyse a controlled set of ground silicon wafers. Optical methods were used to study the strain distribution, scattering-in depth and surface topography of the sample set. Acoustic and X-ray diffraction were used to directly observe variations in the Young's modulus and the lattice constant, respectively. The techniques used ranged from point analysis to whole wafer mapping and averaging. The study indicates that the various physical properties of the lattice damage arise from closely linked processes taking place during the grinding process. The correlations between the methods included in this study have been identified and quantified, and the relationships between the various observable quantities of subsurface damage are discussed.

Rotational grinding is solution to surface damages
Proceedings of SEMICON West 2003, ISBN 1-892568-78-0 (2003).

With the introduction of rotational grinding to the silicon wafer manufacture, either ductile or brittle mechanism may be chosen, displaying different surface characters. Ductilely machined wafer show superior results in terms of roughness and SSD; however, amorphous layers were encountered with these wafers, hinting at high energy levels during machining. Innovative metrology principles are sought for closer analysis of the phenomena observed.

References

1	World Semiconductor Trade Statistics (WSTS) Semiconductor Market Forecast June 2003 www.wsts.org
2	L. Pavesi, J. Phys.: *Condens. Matter* **15** (2003) 1169–1196.
3	P. Van Zant, Microchip Fabrication, McGraw-Hill, New York, 1997 pp. 53-65
4	http://www.bipm.org
5	Hamamatsu Photodiode Technical Information, (Hamamatsu Photonics K. K., Hamamatsu City, Japan)
6	S. M. Sze, Physics of Semiconductor Devices, Wiley, New York, 1981 pp 749-760.
7	J. A. Wahl and S. Tiwari, NNUN Abstracts 2002 / Electronics, p. 37
8	M. Emsley, O. Dosunmu, and M. Ünlü, *IEEE J.Of Sel. Topics In Quantum Electr.*, **8**, 948-955 (2002).
9	B. Yang, J. Schaub, S. Csutak, D. Rogers, and J. Campbell, *IEEE Photonics Tech. Lett.*, **15** 745-747 (2003)
10	F. Hengstberger, "The absolute measurement of radiant power," in Absolute radiometry, F. Hengstberger, ed., Boston, Academic Press 1989, 1-144.
11	The basis of physical photometry, Wien, Commission Internationale de l'Éclairage 1983, CIE publication no. 18.2
12	Goodman T.M., Key P.J., *Metrologia* **25**, 29-40 (1988).
13	Y Ohno and M Navarro, *Metrologia* **35** 317-321 (1998).
14	Toivanen P., Kärhä P., Manoochehri F., Ikonen E., *Metrologia* **37**, 131-140 (2000)
15	J.E. Martin, N.P. Fox and P.J. Key, *Metrologia* **21**, 147 (1985).
16	A. Lassila, H. Hofer, E. Ikonen, L. Liedquist, K. D. Stock and T. Varpula, *Meas. Sci. Technol.* **8**, 123-127 (1997).
17	P. V. Foukal, C. Hoyt, H. Kochling and P. Miller, *Appl. Opt.* **29**, 988 (1990).
18	M. Born and E. Wolf, Principles of Optics, 7th ed., Cambridge University Press, Cambridge, 1999, pp. 40, 632–633.
19	K.D. Mielenz, K.L. Eckerle, R.P. Madden, and J. Reader, "New reference spectrophotometer," *Appl. Opt.* **12**, 1630-1641 (1973).
20	S. Cunsolo, P. Dore and C. P. Varsamnis, *Appl. Opt.* **31,** 4554-4558 (1992).
21	F. Manoochehri and E. Ikonen,"High-accuracy spectrometer for measurement of regular spectral transmittance," *Appl. Opt.* **34,** 3686-3692 (1995).
22	P. Kärhä, A. Lassila, H. Ludvigsen, F. Manoochehri, H. Fagerlund, and E. Ikonen, *Opt. Eng.* **34**, 2611-2618 (1995).
23	F. Manoochehri, A. Haapalinna,and E. Ikonen, *Proceedings of the XIV IMEKO World Congress* **Vol II**, J. Halttunen, Ed.. (Finnish Society of Autromation, Helsinki, Finland 1997 p.108-113.
24	Melles-Griot Laser Beam Measurement Tutorial, Melles-Griot Inc, Carlsbad, CA, USA. http://beammeasurement.mellesgriot.com/tutorial.asp

25   L. P. Boivin, *Metrologia* **30**, 355-360 (1993).

26   R. Köhler, R. Pello and J. Bonhoure, *Appl. Opt.* **29**, 4212-4215 (1990).

27   E. F. Zalewski, C. R. Duda, "Silicon photodiode device with 100% external quantum efficiency," *Appl. Opt.* **22**, 2867 (1983).

28   N. P. Fox, "Trap detectors and their properties," *Metrologia* **28**, 197-202 (1991).

29   P. Kärhä, A. Lassila, H. Ludvigsen, F. Manoochehri, H. Fagerlund and E. Ikonen, *Opt. Eng.* **34**, 2611-2618 (1995).

30   T.R. Gentile, J. M. Houston and C.L. Cromer, Appl. Opt., 35, 4392-4403 (1996)

31   J. Gran and A. S. Sudbø, *Metrologia* **41**, 204-212 (2004).

32   P. Kärhä, T. Kübarsepp, F. Manoochehri, P. Toivanen, E. Ikonen, R. Visuri, L. Ylianttila, and K. Jokela , *J. of Geoph. Res* (1998)

33   T. Kübarsepp, P. Kärhä, and E. Ikonen, *Appl. Opt.* **39**, 9-15 (2000).

34   T. Kübarsepp, H.W. Yoon, S. Nevas, P. Kärhä, and E. Ikonen, *Metrologia* **39**, 399-402 (2002).

35   E. Ikonen, P. Kärhä, A. Lassila, F. Manoochehri, H. Fagerlund and L. Liedquist, *Metrologia* **32**, 689-692 (1995/96).

36   P. Kärhä, P. Toivanen, F. Manoochehri, and E. Ikonen, *Appl. Opt,.* **36**, 8909-8918 (1997).

37   S. Ippolito,B. Goldberg, and M. S. Ünlü, *Appl. Phys. Lett*, 4071-4073 (2001)

38   G. Harbeke and M.J. Schultz (Eds.), Semiconductor Silicon, Springer, Berlin, 1989

39   A. Rosencwaig, J. Opsal, and D. L. Willenborg, *Appl. Phys. Lett.* **43**, 166 (1983)

40   A. Ehlert, M. Kerstan, H. Lundt, A. Huber, D. Helmreich, H. Geiler, H. Karge and M. Wagner, *Opt. Eng.* **36** 446-458 (1997).

41   H. Tönshof, W. Schmieden, I. Inasaki, W. König, G. Spur, Annals of the CIRP 39/2 621 (1990).

42   C. Menz, Randzonenanalyse bearbeiteter Silizium-Oberflächen. VDI Verlag, Düsseldorf, 1997, in German.

43   Z.J. Pei, S.R. Billingsley and S. Miura, *Int. Journal of Machine tools and Manufacture* **39**, 1103-1116 (1999)

44   P. Fisher and R.E.M. Vickers, *App. Phys. Letters* **79**, 3458-3460 (2001)

45   Y Gogotsi, C Baek and F Kirscht, *Semicond. Sci. Technol.* **14** 936-944 (1999)

46   Zhang, J.M., Sun, J.G., and Pei, Z.J., *CD-ROM Proceedings of the International Mechanical Engineering Congress and Exposition 2003*, Washington, DC, November 16-21 (2003).